# Seasonal Prediction of European Spring Precipitation from ENSO and Local Sea Surface Temperatures

(Short title: Seasonal Prediction of European Spring Precipitation)

BENJAMIN LLOYD-HUGHES[1] and MARK A. SAUNDERS[1,2]

[1]Department of Space and Climate Physics, University College London,

Holmbury St. Mary, Dorking, Surrey RH5 6NT, U.K..

(Email: blh@mssl.ucl.ac.uk; Tel: 01483 204292; Fax: 01483 278312)

**Submitted to International Journal of Climatology**

**April 11, 2001**

**Revised**

**August 8, 2001**

**Accepted**

**August 14, 2001**

[2] Benfield Greig Hazard Research Centre, University College London,

Gower Street, London, WC1E 6BT.

# Abstract

The extent to which European seasonal precipitation is predictable is a topic of scientific and societal importance. Although the potential for seasonal prediction is much less over Europe than in the tropics it is not negligible. Previous studies suggest that European seasonal precipitation skill may peak in the spring (March-April-May) period, this being the season when ENSO teleconnections to the north Atlantic and European sector are at their strongest. Examination of the correlation significance and temporal stability of contemporaneous and lagged ENSO links to European and north African precipitation over 98 years confirms this to be the case. The strongest ENSO links are found across the Central European (CE) region [45$^o$N-55$^o$N, 35$^o$E-5$^o$W]. These links are symmetric with the sign of ENSO. Using a linear statistical model employing temporally stable lagged ENSO and lagged local north Atlantic sea surface temperatures as predictors, we compute the forecast skill and significance of CE spring precipitation over 30 independent years. For early March forecasts our model skill is 14-18% better than climatology which is significant at the 95% level.



Keywords: ENSO, Europe, forecast, precipitation, seasonal, SST.

# 1 Introduction

The long-range forecasting of seasonal mean rainfall is attracting increasing interest as society, industry and government attempt to minimise the risk, uncertainty and financial volatility associated with unseasonal weather. Seasonal prediction is based upon the premise that the lower atmosphere is forced by large-scale anomalous surface processes. Since these surface forcings evolve at a slower rate than the weather systems of interest they can be used to predict anomalies in large scale atmospheric behaviour over long (seasonal) periods of time (*e.g.* Gilchrist 1986, Barnston & Smith 1996, Rowell 1998, Anderson 2000). Recent assessments of seasonal precipitation predictability using coupled general circulation models (*e.g.* Branković & Palmer 2000, Graham *et al.* 2000, Doblas-Reyes *et al.* 2000) indicate that skillful forecasts may be possible for northern extratropical regions. Whilst the potential for prediction is much lower than that found for the tropics, it is generally not negligible and is seen to peak around the spring March-April-May (MAM) period (Branković *et al.* 1994, Doblas-Reyes *et al.* 2000, Graham *et al.* 2000). Predictability is found to be higher in ENSO extreme years (Branković & Palmer 2000), implying that at least part of the available skill can be attributed to forcing from the tropical Pacific ocean.

The influence of ENSO on European climate has been discussed by many authors, with the review articles by Moron & Ward (1998) and Fraedrich (1994) providing a good introduction. On a more regional scale, Wilby (1993) relates changes in weather type over the British Isles to ENSO activity. Concerning precipitation, the most promising finding is that identified by Kiladis & Diaz (1989) between

wintertime ENSO and springtime rain in Europe. van Oldenborgh *et al.* (2000) demonstrate the statistical significance of this relationship for the period 1857-1998. They find that it explains 24% of the variance in MAM precipitation over the region $47.5^o$N - $52.5^o$N, $35^o$E-$5^o$W.

Whilst the effect of ENSO on European seasonal precipitation appears significant, local climate factors may also be important. In particular, anomalous sea surface temperatures (SSTs) over the North Atlantic are thought to influence European seasonal weather (*e.g.* Czaja & Frankignoul 1999, Drévillon *et al.* submitted, 2001). Colman & Davey (1999) describe an empirical forecast scheme for summer temperature, rainfall, and pressure in Europe based on wintertime north Atlantic SSTs.

Two broad types of prediction model - dynamical and statistical - are employed in current seasonal forecasts. While dynamical prediction schemes should, in theory, eventually be superior to statistical models, this is not the case at present. Studies assessing current capabilities of the two model types show that the best statistical models are as good as, if not better, than the best dynamical seasonal models (Barnston *et al.* 1999, Anderson *et al.* 1999, Landsea & Knaff 2000). Furthermore, this situation has not changed in recent years (Barnston *et al.* 1999). A recent analysis of the performance of 12 real-time seasonal forecasting schemes during the strong 1997-98 El Niño found that the best performing model for forecasting the entirety of the event was the statistical ENSO-CLIPER model (Landsea & Knaff 2000).

This paper describes a statistical forecasting scheme for MAM central Euro-

pean precipitation based on significant lagged relationships to wintertime ENSO and North Atlantic SST. Primary emphasis is placed on predictor stability. Model performance is assessed over thirty years of independent data. Section 2 describes the methodology, including the data, predictor selection, predictor stability, and model skill assessment. Section 3 presents the results from two models, one based solely on ENSO, the other combining ENSO and local SST predictors. Section 4 discusses the results, and conclusions are drawn in Section 5.

# 2 Methodology

## 2.1 Data

Gridded precipitation data are taken from the monthly 0.5 degree set compiled by the Climatic Research Unit at the University of East Anglia (New *et al.* 2000). These data cover the period 1901-1998. Gridded SST data for 1901-1949 are taken from the monthly 5.0 degree United Kingdom Met Office Global Ice and Sea Surface Temperature (GISST) data set version 2.3b [which is an update of version 2.2 (Rayner *et al.* 1996)], and for 1950-1998 from the monthly 2.5 degree NCEP/NCAR global reanalysis data set (Kalnay *et al.* 1996, Kistler *et al.* 2001). The ENSO NINO3 SST index we employ comes from the SST reconstruction of Kaplan *et al.* (1998).

## 2.2 Prediction Model

We employ a simple linear regression model comprising a set of k parameters ($a_{0,1,\ldots,k}$) which relate one or more predictors ($x_{1,2,\ldots,k}$) to a single predictand ($y$):

$$y = a_0 + a_1 \cdot x_1 + a_2 \cdot x_2 + \cdots + a_k \cdot x_k \tag{1}$$

Stability in time is fundamental to the utility of any empirical forecast scheme. In this study, predictor-predictand relationships are deemed to be temporally stable if they are statistically robust over the period 1901-1998, as well as over the two sub-periods 1901-1949 and 1950-1998. This is formalised by use of the Chow test statistic as used in economics (Chow 1960, Stewart 1991):

$$Chow = \frac{SSE_C - (SSE_1 + SSE_2)}{k} \Big/ \frac{SSE_1 + SSE_2}{L - 2k} \tag{2}$$

This is F-distributed and measures the ratio of the sum of the squares obtained from the full regression ($SSE_C$) against the sum of the squares obtained from two adjacent subsets of the data ($SSE_{1,2}$), where the two subsets combine to form the whole series of length L.

Any change in the regression parameters ($a_{0,1,..k}$) over time will result in an increase in $SSE_c$ relative to $SSE_{1,2}$. Thus we test whether the parameters remain constant over time. Specifically, we examine the null hypothesis (that the regression coefficients are the same for both subsets of the data), against the alternative hypothesis (that the regression coefficients are not the same for both subsets of the data). Failure to reject the null hypothesis (at some specified level) is taken to imply stability. Relationships which yield F-probabilities of greater than 5% are considered to be stable.

## 2.3 Skill Assessment

### 2.3.1 Separate Training and Forecast Intervals

The firm separation of training and forecast periods is fundamental for true skill assessment. This distinction ensures that hindcasts are applied always to independent data, thus making the model skill the true forecast skill. We achieve this separation by using an initial training period of 1901-1968, leaving 1969-1998 (30 years) for model forecast assessment. The training period increases one year at a time as each forecast is made. For example, an independent forecast for 1969 is built using 1901-1968 data to identify the potential predictors and compute the regression coefficients. Similarly, an independent forecast for 1970 is trained using data up to and including 1969, and so on.

### 2.3.2 Skill Measures

Several methods are in common use to assess the skill of forecast models (*e.g.* Wilks 1995, von Storch & Zwiers 1999). We employ the percentage of variance explained (PVE), the percentage improvement in mean absolute error over a climatological forecast ($\mathrm{MAE}_{cl}$), and the percentage improvement in root mean square error over a climatological forecast ($\mathrm{RMSE}_{cl}$). The $\mathrm{RMSE}_{cl}$ and $\mathrm{MAE}_{cl}$ skill measures are the most robust. Climatology is taken as the long term average prior to each year being forecast.

### 2.3.3 Statistical Confidence of Model Skill

We compute confidence intervals on our forecast skill using the bootstrap method (Efron 1979; also see *e.g.* Efron & Gong 1983, LePage & Billiard 1992, Wilks 1995). This tests the hypothesis that the model forecasts are more skillful than those from climatology to some level of significance. We apply the bootstrap by randomly selecting (with replacement) thirty predictand (or actual) values from the original thirty hindcast years. This provides a new set of hindcasts for which each verification measure ($\mathrm{RMSE}_{cl}$, $\mathrm{MAE}_{cl}$ and PVE) can be calculated. This process is repeated many times (25,000 in this case) and the results histogrammed to give the required distributions. Provided that the original data points are independent (in distribution and order), the distribution of these recalculated parameters maps the uncertainty in the forecast skill about the original value. 95% two-tailed confidence intervals for this uncertainty are then readily obtained.

### 2.3.4 Other Considerations

Other considerations which will help users make effective use of forecasts include information on *forecast bias* (the correspondence between the average forecast and the average observed value), and *forecast sharpness* (the characteristic where forecasts which show little deviation from climatology are said to possess 'low sharpness', whereas forecasts which often differ significantly from climatology are described as being 'sharp').

## 2.4 Predictor and Predictand Selection

### 2.4.1 Stability of the ENSO teleconnection

Following van Oldenborgh *et al.* (2000), ENSO is represented by the NINO3 region [$5^o$S-$5^o$N, $90^o$W-$150^o$W] SST index. Figure 1a shows the Pearson product moment correlation coefficients ($r$)of the December-January-February (DJF) average NINO3 and March-April-May (MAM) precipitation over Europe (1901-1998). Significance, assessed using Student's t-test against the null hypothesis of no correlation, is shown by shading at the 5% and 1% levels. The areas of significant lagged correlation are in good accordance with previous studies (*e.g.* Kiladis & Diaz 1989, van Oldenborgh *et al.* 2000). Significant positive correlations are observed in a band crossing Central Europe from England and Wales to the northern Black Sea. Significant negative correlations are present over north Africa and in southeast Spain.

Figure 1b, and Figure 1c illustrate spatial correlations obtained by regressing $\text{NINO3}_{DJF}$ (the subscript representing the season) onto MAM precipitation for the sub-periods 1901-1949 and 1950-1998 respectively. Considerable variation is seen between the two panels. In the first half of the twentieth century, significant positive correlations are found across Bulgaria, Romania, Hungary, and Poland, extending westward into Germany. Significant negative correlations are evident over Algeria and northeast Morocco. The same north-south dipole-like response of European rainfall anomaly to ENSO is also seen in the latter half of the twentieth century, with positive correlations to the north, and negative correlations to the south. However, the positive centre is displaced westward into the Netherlands, northern France, England, and Wales. A second positive centre is located across the Ukraine, ex-

tending north into Russia, and southwest to the Caspian Sea. The negative centre previously found over Algeria, is now displaced northwest over Morocco and into southeast Spain.

Such spatial instability severely limits the potential for predictability over small areas. The study by Koster & Suarez (1995) indicates that ocean variability has a stronger influence on precipitation when the latter is averaged over larger spatial scales. Examining Figure 1, suggests two possible regions suitable for agglomeration. The first comprises the region [45$^o$N-55$^o$N, 35$^o$E-5$^o$W] spanning central Europe and encompassing a land area of 5 x $10^6$ km$^2$. Precipitation over this region will henceforth be referred to as Central European Precipitation (CEP). This region is similar to that studied by van Oldenborgh *et al.* (2000) but covers twice the meridional area. Whilst the pattern correlation between the CEP subsections of Figures 1b and 1c is negligible ($r = 0.02$), the correlations for the area averaged quantity CEP$_{MAM}$ versus NINO3$_{DJF}$ are $r = 0.52$ (1901-1949) and $r = 0.45$ (1950-1998). A bootstrapped estimate of the error on the correlation for the period 1901-1998 gives a 95% confidence range of 0.33 to 0.62. A second study area is defined to cover the extreme northwest of Africa. This comprises the region [30$^o$N-35$^o$N, 15$^o$E-10$^o$W], a land area of 1.3x$10^6$ km$^2$. Precipitation over this second region will henceforth be termed Northwest African Precipitation (NAP).

In a comprehensive analysis, CEP and NAP were regressed onto NINO3 for all seasons at lags of 0, 3, 6, and 9 months, for the period 1901-1998. The results are displayed in Figure 2a for CEP, and in Figure 2b for NAP. A peak in correlation is observed between CEP spring (CEP$_{MAM}$) and NINO3 at a lag of 3 months (i.e.

NINO3$_{DJF}$) at $r$=0.49. This result is almost identical to that reported by van Oldenborgh *et al.* (2000). A similar correlation influence (but of opposite sign) is observed between NAP$_{MAM}$ and NINO3$_{DJF}$, with $r$=-0.47. A secondary correlation peak is seen between the autumn season September-October-November NAP (NAP$_{SON}$) and the NINO3 summer June-July-August (NINO3$_{JJA}$) index, with $r$=0.24. The NAP results are similar to those reported by Rodo *et al.* (1997) for station data across southeast Spain.

The parameter temporal stability of these results, as judged by the Chow test, are presented in Table 1. It can be seen that the CEP$_{MAM}$-NINO3$_{DJF}$ relationship is the most stable of the ENSO teleconnection influences on European seasonal precipitation. The corresponding NAP relationship is less stable, *i.e.* with a Chow value of 1.75 we can reject the null hypothesis (that the regression parameters are constant in time) at the 18% level. Possible temporal instability in NAP was suspected by Ropelewski & Halpert (1987), and reported by Rodo *et al.* (1997). Inspection of Figure 1, suggests this result is not surprising considering the large spatial variation within the small area encompassed by NAP. The NAP$_{SON}$-NINO3$_{JJA}$ relationship is stable, but as it accounts for only a small (6%) fraction of the seasonal variance in rainfall, it is unlikely to be useful for predictive purposes.

As an aside, it is worthwhile to comment on a further teleconnection between ENSO and late summer precipitation over southern Iberia. Defining the southern Iberian region as [35$^o$N-40$^o$N, 0$^o$W-5$^o$W] and taking the area average, we construct a measure representative of rainfall in this region. Correlating this with NINO3 for JAS 1950-1996 gives $r$ = 0.61. Incorporating data for the strong El Niño of

1997, causes this to rise to $r = 0.66$. This contrasts with $r = -0.15$ for the period 1901-1949. Considering the long record 1901-1998 gives $r = 0.25$, the Chow value for this period is 8.1 (F-prob=0.001) indicating severe temporal instability. The Chow values for the two sub-periods indicate stability within themselves. Thus, depending on the length of record available, we conclude either: (1) There is a strong, stable relationship between precipitation in late summer over southern Iberia and concurrent sea surface temperature in the equatorial Pacific (most recent 50 years of data); or (2) The summer southern Iberian teleconnection is weak and unstable (100 years of data). This example illustrates the need for long period records when assessing the utility of such relationships for predictive purposes.

### 2.4.2 Symmetry of the ENSO teleconnection

Implicit in the use of linear regression is the assumption of a symmetrical response in the predictand to predictors of opposite sign. To investigate the symmetry of the MAM precipitation response to El Niño and La Niña events, the data were partitioned into years corresponding to the ten highest and ten lowest values of the $\text{NINO3}_{DJF}$ index for each half of the century. This facilitates a comparison of the location and strength of the response to each type of event. Figures 3a-3d show the resultant MAM average precipitation anomaly fields for each of the four composites. The anomalies are relative to the long term seasonal average for the whole century.

In general the patterns are symmetric in both location and magnitude within each half century, but not between the two halves. It is noteworthy that the response in the first half century is slightly stronger in La Niña years, whilst in the latter half century, the response is slightly stronger in El Niño years. The observed shifts in

the centres of action closely resemble those seen in the correlation maps shown in Figure 1. The close correspondence between patterns of opposite extrema supports the view that the ENSO teleconnection influence on European spring precipitation is symmetric with the sign of ENSO and that the use of linear regression is appropriate.

### 2.4.3 Local SST

The strength and consistency of the relationship between $\text{NINO3}_{DJF}$ and $\text{CEP}_{MAM}$ suggests it represents something more than a random statistical association. However, the proportion of the $\text{CEP}_{MAM}$ variance 1901-1998 which can be explained by equatorial Pacific SST is only 24%. The model study of Davies *et al.* (1997) and the empirical work of Folland & Woodcock (1986), suggest that additional long-range predictability may be available over European coastal regions by including the direct effect of adjacent SST anomalies. The work of Czaja & Frankignoul (1999) and Drévillon *et al.* (submitted, 2001) suggest that anomalies in the North Atlantic atmospheric circulation may be related to previous SST conditions in the North Atlantic.

Local effects are investigated in isolation from the ENSO response by constructing a new precipitation time series, $\text{CEP}'_{MAM}$ from the residuals generated when $\text{NINO3}_{DJF}$ is regressed onto $\text{CEP}_{MAM}$. Spatial correlation maps between this residual error series and the MAM concurrent North Atlantic SST, are shown in Figure 4. The ENSO-only model over predicts when SST is cooler than normal in the North Sea, Bay of Biscay, and Western Mediterranean, and *vice versa*. Whilst this contemporaneous observation is interesting, it is of little practical value in forecasting precipitation unless it too can be reliably predicted. Indeed, we may simply be

observing the oceanic response to the same anomalies in the atmospheric circulation which are giving rise to the precipitation fields of interest.

Figure 5 shows the correlation relationship between the $\mathrm{CEP}'_{MAM}$ residual error series above, and the December-January-February lagged North Atlantic SST, $\mathrm{SST}_{DJF}$, for each half of the twentieth century. Stable correlations are observed in waters west of the British Isles, extending southward along the coast of Portugal and North Africa. A local SST index (LSST) is defined as the area average SST in the region [40$^o$N-60$^o$N, 10$^o$W-20$^o$W] west of Ireland. $\mathrm{LSST}_{DJF}$ correlates at $r$=-0.28 with $\mathrm{CEP}'_{MAM}$. The correlation between $\mathrm{LSST}_{DJF}$ and $\mathrm{CEB}'_{MAM}$ is -0.21 for the period 1901-1949 and -0.36 for the period 1950-1998. A bootstrapped estimate of the error on the correlation for the period 1901-1998 gives a 95% confidence range of -0.09 to -0.46.

The Atlantic region encompassed by LSST exhibits significant decadal trend. It is possible that much of the observed correlation could arise (misleadingly) from monotonic changes in both $\mathrm{LSST}_{DJF}$ and $\mathrm{CEB}'_{MAM}$ attributable to decadal trend. A low pass filter with a cut-off frequency of 10 years was used to estimate the low frequency component for each time series, which was then subtracted from the raw data. The correlation was repeated using the detrended data and found to be -0.24, thus implying that the majority of the correlation between $\mathrm{LSST}_{DJF}$ and $\mathrm{CEB}'_{MAM}$ arises from interannual covariability and not from decadal trend.

$\mathrm{LSST}_{DJF}$ is also almost independent from ENSO ($r$($\mathrm{LSST}_{DJF}$,$\mathrm{NINO3}_{DJF}$)=-0.1). The $\mathrm{CEP}'_{MAM}$-$\mathrm{LSST}_{DJF}$ relationship has a Chow value of 0.43 with a corresponding F-probability of 0.65. Such a high F-probability is a firm indication that

the relationship is temporally stable. We note that LSST is similar to the Region 3 defined by Folland & Woodcock (1986) in their experimental mean sea level pressure forecasts for the United Kingdom.

## 2.5 Results

Given the near statistical independence of the two influences on $\mathrm{CEP}_{MAM}$ identified above, it is reasonable to construct a multiple linear regression of $\mathrm{NINO3}_{DJF}$ and $\mathrm{LSST}_{DJF}$ onto $\mathrm{CEP}_{MAM}$ for the period 1901-1998.

The parameters $a_{1,2}$, corresponding to the predictors $\mathrm{NINO3}_{DJF}$ and $\mathrm{LSST}_{DJF}$, together with their standard errors and significances are summarised in Table 2. It can be seen that both parameters and the constant ($a_o$) are significant at the 1% level (tested against the null hypothesis of $a_k = 0$). This regression explains over 30% of the variance in $\mathrm{CEP}_{MAM}$ 1901-1998. Analysis of the residuals from this regression shows them to be normally distributed, homoscedastic, and devoid of significant auto-correlation; characteristics satisfying the requirements for linear regression.

The level of the variance explained by the combined influence of $\mathrm{NINO3}_{DJF}$ and $\mathrm{LSST}_{DJF}$ may be sufficiently high to be useful for seasonal forecasting. Nicholls (1984) hypothesises that given the potential non-stationarity within predictor-predictand time series, the optimum training period to use in deriving a predictive equation may not be that which contains all the available data. This question was examined using hindcasts with training periods of length n, ranging from 10 to 68 years. For each n, we made 30 independent predictions of $\mathrm{CEP}_{MAM}$ covering the period 1969-1998;

*e.g.* for n=10 we use 1988-1997 data to predict 1998, we use 1987-1996 data to predict 1997, and so on back to 1969. Each set of predictions was then compared with the corresponding set of observations. Statistics were calculated for bias, root mean square error (RMSE), mean absolute error (MAE), and correlation ($r$), as defined in the standard way (Wilks 1995) These are shown as a function of n in Figure 6. The gradual improvement seen in all the statistics as the training period increases, is indicative of stability and suggests that the regression parameters are asymptotically approaching values representative of the complete population. RMSE tends to a value of about 18mm, MAE tends to 15mm and the correlation coefficient tends to $r \approx 0.55$. Model bias is always small (less than 4mm), peaking at 3.5mm for a training period of 23 years.

A final set of thirty year hindcasts 1969-1998 were performed for the $\mathrm{NINO3}_{DJF}$ and $\mathrm{LSST}_{DJF}$ regression model using all the available training data.This was achieved by extending the training period by one year as new data became available. Thus, 1969 was predicted using a model trained on 1901-1968 data, 1970 was predicted using a model trained on 1901-1969 data, *etc.*. The results are shown as a scatter plot of predicted versus actual values in Figure 7. The graph is divided into four quadrants relative to the $\mathrm{CEP}_{MAM}$ climatology 1961-1990. Table 3 summarises the $\mathrm{CEP}_{MAM}$ seasonal forecast skill both for the above model and, for comparison, the $\mathrm{NINO3}_{DJF}$ only model.

# 3 Discussion

From Figure 7 and Table 3 it can be seen that whilst our early March $\text{CEP}_{MAM}$ forecast models are not *sharp*, nor particularly *accurate*, they exhibit useful skill which is 14-18% better than climatology. From Table 3 it can be seen that the combined $\text{NINO3}_{DJF}$-$\text{LSST}_{DJF}$ model improves upon the skill of the $\text{NINO3}_{DJF}$ model. However, it is clear that most of the skill in both models comes from the two well predicted El Niño extreme years of 1983 and 1998. When the 30-year hindcasts are repeated with the 1983 and 1998 strong ENSO years removed, the $\text{NINO3}_{DJF}$ and $\text{LSST}_{DJF}$ model skill falls to 8% ($\text{RMSE}_{cl}$) and 4% ($\text{MAE}_{cl}$), while the $\text{NINO3}_{DJF}$ only model skill falls to 7% ($\text{RMSE}_{cl}$) and 3% ($\text{MAE}_{cl}$). Thus the ENSO extreme years are contributing $\sim$10% of the 14-18% objective skill improvement over climatology.

Histograms of the bootstrapped values of $\text{RMSE}_{cl}$ and $\text{MAE}_{cl}$ are shown in Figure 8 for the $\text{NINO3}_{DJF}$ and $\text{LSST}_{DJF}$ model. The model deterministic skill scores are shown by the solid vertical lines, and the 95% confidence intervals are marked by the dashed vertical lines. The latter are also shown in Table 3. They demonstrate that the hindcast skill values are significant at close to the 95% confidence level. This result is reinforced by the vast majority of the 25,000 skill score realisations being positive (95% for $\text{RMSE}_{cl}$ and 87% for $\text{MAE}_{cl}$). Given the unbounded nature of the skill scores, this is firm evidence that the forecast scheme possesses real skill. We also note that both distributions are skewed slightly towards negative values. This skewness is an artifact of the skill score measures. For example, if we consider $\text{RMSE}_{cl}$, its positive values are constrained to a maximum value of 100%, while

its negative values are not and will tend to negative infinity for forecasts far worse than climatology. These different tendencies give rise to the skewed distribution of $\mathrm{RMSE}_{cl}$, and similarly for $\mathrm{MAE}_{cl}$.

The basic mechanism for the interaction between ENSO and European precipitation is poorly understood. Until this understanding improves, a thorough assessment of the utility of the results presented here can not be made. However, it is known that ENSO exerts a positive forcing on tropical north Atlantic SSTs and this effect is strongest in boreal spring (MAM) (Enfield & Mayer 1997). Thus, the ENSO influence on $\mathrm{CEP}_{MAM}$ may be an extension of this influence. More than one physical mechanism has been proposed to explain the ENSO teleconnection to the tropical north Atlantic. The favoured mechanism involves anomalous Walker circulation leading, during warm (cold) ENSO phases, to increased (decreased) subsidence over the tropical north Atlantic, and to warming (cooling) of the underlying SSTs (Kidson 1975, Saravanan & Chang 2000, Sutton *et al.* 2000). An alternative mechanism invokes the propagation of Rossby-like wave disturbances via the extratropics into the northwest tropical Atlantic (Nobre & Shukla 1996). Other studies supporting a dynamical basis for an ENSO influence on European climate include the conceptual work of Bjerknes (1966), and modelling studies by Davies *et al.* (1997) and Venzke *et al.* (1999). Bjerknes [*ibid*] describes how ENSO modulates the Aleutian Low which in turn leads to large scale effects downwind. The Aleutian Low, and its effect on high latitude circulation, is known to vary on a decadal scale (Overland *et al.* 1999). Increased understanding of such processes may well clarify the response of European MAM precipitation to ENSO forcing, and thus, lead to more

reliable seasonal forecasts over better defined areas. Dynamical studies using coupled GCMs with prescribed SSTs are likely to play an important role in increasing this understanding.

# 4 Conclusions

Partitioning the data in time and by the phase of ENSO reveals changes, over the first and second halves of the twentieth century, in the response of the European precipitation field to forcing by SST anomalies in the equatorial Pacific. Large scale area averaging yields temporally stable relationships, but only at the expense of spatial resolution. Results from an empirical model show that up to 30% of the variance in springtime precipitation over the region [45$^o$N-55$^o$N, 35$^o$E-5$^o$W] can be predicted beforehand using a combination of ENSO and local North Atlantic SST forcings. This is close to the maximum predictable atmospheric variance over Europe found by model studies examining the relative magnitudes of SST forced atmospheric variability to internal (unpredictable) atmospheric variability (*e.g.* Koster & Suarez 1995, or Davies *et al.* 1997).

We find that spring is the most predictable season for European precipitation. This supports dynamical model studies which show less ensemble spread and thus less internal atmospheric variability in the spring (*e.g.* Branković *et al.* 1994). Objectively, this equates to an improvement of around 18% (14%) in RMSE (MAE) over a climatological forecast when predicting March-April-May precipitation across central Europe from wintertime SSTs. Confidence intervals, estimated by the bootstrap method, show that this skill is significant at around the 95% level.

Although it is easy to think of people who would be interested in a seasonal forecast for a point, or even a country, it is difficult to envisage the use for a forecast spanning an area of as large as 5 x $10^6$ $km^2$ as the CEP region. It is unfortunate that this appears to be the scale required to obtain stable statistical predictive relationships for European seasonal precipitation.

Acknowledgements

Benjamin Lloyd-Hughes is supported by a Research Studentship from the UK Natural Environment Research Council. He gratefully thanks St. Paul Re. for industrial CASE sponsorship. We acknowledge helpful discussions with Paul Rockett and comments by Geert Jan van Oldenborgh. The NCEP/NCAR global reanalysis project data are provided by NOAA-CIRES, Climate Diagnostics Centre, Boulder, Colorado, USA.

# References


Anderson D. 2000. Bright future for seasonal forecasts. *Physics World*. **10**:43–48.

Anderson J, van den Dool H, Barnston A, Stern WCW, Ploshay J. 1999. Present-day capabilities of numerical and statistical models for extratropical seasonal simulation and prediction. *Bulletin of the American Meteorological Society*. **7**:1349–1361.

Barnston AG, H.Glantz M, He Y. 1999. Predictive skill of statistical and dynamical climate models during the 1997-98 El Niño episode and the 1998 La Niña onset. *Bulletin of the American Meteorological Society*. **80**:217–243.

Barnston AG, Smith TM. 1996. Specification and prediction of global surface temperature and precipitation from global SST using CCA. *Journal of Climate*. **9**:2660–2697.

Bjerknes J. 1966. A possible response of the atmospheric Hadley circulation to equatorial anomalies of ocean temperature. *Tellus*. **18**:820–829.

Branković C, Palmer TN. 2000. Seasonal skill and predictability of ECWMF PROVOST ensembles. *Quarterly Journal of the Royal Meteorological Society*. **126**:2035–2067.

Branković C, Palmer TN, Ferranti L. 1994. Predictability of seasonal atmospheric variation. *Journal of Climate*. **7**:217–237.

Chow GC. 1960. Tests of equality between sets of coefficients in two linear regressions. *Econometrica*. **28**:591–605.

Colman A, Davey M. 1999. Prediction of summer temperature, rainfall, and pressure in Europe from preceding winter North Atlantic ocean temperature. *International Journal of Climatology*. **19**:513–536.

Czaja A, Frankignoul C. 1999. Influence of the north Atlantic SST on the atmospheric circulation. *Geophysical Research Letters*. **26**:2969–2972.

Davies JR, Rowell DP, Folland CK. 1997. North Atlantic and European seasonal predictability using an ensemble of multidecadal atmospheric GCM simulations. *International Journal of Climatology*. **17**:1263–1284.

Doblas-Reyes FJ, Déqué M, Piedelievre J. 2000. Multi-model spread and probabilistic seasonal forecasts in PROVOST. *Quarterly Journal of the Royal Meteorological Society*. **126**:2069–2087.

Drévillon M, Terray L, Rogel P, Cassou C. submitted, 2001. Mid latitude SST influence on European winter climate variability in the NCEP Reanalysis. *Climate Dynamics*.

Efron B. 1979. Bootstrap methods: another look at the jackknife. *The Annals of Statistics*. **7**:1–26.

Efron B, Gong G. 1983. A leisurely look at the bootstrap, the jackknife, and cross-validation. *The American Statistician*. **37**:36–48.

Enfield DB, Mayer DA. 1997. Tropical Atlantic SST variability and its relation to El Niño Southern Oscillation. *Journal of Geophysical Research*. **102**:929–945.

Folland CK, Woodcock A. 1986. Experimental monthly long-range forecasts for the United Kingdom. Part 1. Description of the forecasting system. *The Meteorological Magazine*. **115**:301–318.

Fraedrich K. 1994. An ENSO impact on Europe? *Tellus*. **46A**:541–552.

Gilchrist A. 1986. Long-range forecasting. *Quarterly Journal of the Royal Meteoro-*

*logical Society*. **112**:567–592.

Graham RJ, Evans ADL, Mylne KR, Harrison MSJ, Robertson KB. 2000. An assessment of seasonal predictability using atmospheric general circulation models. *Quarterly Journal of the Royal Meteorological Society*. **126**:2211–2240.

Kalnay E, Kanamitsu M, and coauthors. 1996. The NCEP/NCAR 40-year Reanalysis Project. *Bulletin of the American Meteorological Society*. **77**:437–471.

Kaplan A, Cane MA, Kushnir Y, Clement AC, Blumenthal MB, Rajagoplalan B. 1998. Analyses of global sea surface temperature 1856-1991. *Journal of Geophysical Research*. **C9**:18,567–18,589.

Kidson JW. 1975. Tropical eigenvector analysis and the southern oscillation. *Monthly Weater Review*. **103**:187–196.

Kiladis GN, Diaz HF. 1989. Global climatic anomalies associated with extremes in the Southern Oscillation. *Journal of Climate*. **2**:1069–1090.

Kistler R, Kalnay E, and coauthors. 2001. The NCEP/NCAR 50-year Reanalysis: monthly means CD-ROM and documentation. *Bulletin of the American Meteorological Society*. **82**:247–267.

Koster RD, Suarez MJ. 1995. Relative contributions of land and ocean processes to precipitation variablility. *Journal of Geophysical Research*. **D7**:13,775–137,990.

Landsea CW, Knaff JA. 2000. How much skill was there in forecasting the very strong 1997-98 el niño? *Bulletin of the American Meteorological Society*. **81**:2107–2119.

LePage R, Billiard L. 1992. *Exploring the Limits of the Bootstrap*. Wiley and Sons.

Moron V, Ward WMN. 1998. ENSO teleconnections with climate variability in the European and African sectors. *Weather*. **53:9**:287–295.

New M, Hulme M, Jones P. 2000. Representing twentieth-century space-time climate variability, part II: Development of 1901-96 monthly grids of terrestrial surface climate. *Journal of Climate*. **13**:2217–2238.

Nicholls N. 1984. The stability of empirical long range forecast techniques: A case study. *Journal of Climate and Applied Meteorology*. **23**:143–147.

Nobre P, Shukla J. 1996. Variations of sea surface temperature, wind stress, and rainfall over the tropical Atlantic and south America. *Journal of Climate*. **9**:2464–2479.

Overland JE, Adams JM, Bond NA. 1999. Decadal variability of the Aleutian low and its relation to high latitude circulation. *Journal of Climate*. **12**:1542–1548.

Rayner NA, Horton EB, Parker DE, Folland CK, Hackett RB. 1996. *Version 2.2 of the Global sea-Ice and Sea Surface Temperature data set, 1903-1994*. CRTN 74, Hadley Centre for Climate Prediction and Research, Meteorological Office, London Road, Bracknell, Berkshire, RG12 2SY. 21 pp plus figures.

Rodo X, Baert E, Comin FA. 1997. Variations in seasonal rainfall in southern Europe during the present century: Relationships with the north Atlantic Oscillation and the El Niño-Southern Oscillation. *Climate Dynamics*. **13**:275–284.

Ropelewski CF, Halpert MS. 1987. Global and regional scale precipitation patterns associated with the El Niño/Southern Oscillation. *Monthly Weather Review*. **115**:1606–1626.

Rowell DP. 1998. Assessing potential seasonal predictibility with an ensemble of multidecadal GCM simulations. *Journal of Climate*. **11**:109–120.

Saravanan R, Chang P. 2000. Interaction between tropical Atlantic variability and El Niño-Southern Oscillation. *Journal of Climate*. **13**:2177–2194.

Stewart J. 1991. *Econometrics*. Philip Allan: New York.

Sutton RT, Jewson SP, Rowell DP. 2000. The elements of climate variability in the tropical Atlantic region. *Journal of Climate*. **13**:3261–3284.

van Oldenborgh GJ, Burgers G, Klein Tank A. 2000. On the El Niño teleconnection to spring precipitation in Europe. *International Journal of Climatology*. **20**:565–574.

Venzke S, Allen MR, Sutton RT, Rowell DP. 1999. The atmospheric response over the north Atlantic to decadal changes in sea surface temperature. *Journal of Climate*. **12**:2562–2584.

von Storch H, Zwiers FW. 1999. *Statistical Analysis in Climate Research*. Cambridge University Press: Cambridge.

Wilby R. 1993. Evidence of ENSO in the synoptic climate of the British Isles since 1880. *Weather*. **48**:234–239.

Wilks DS. 1995. *Statistical Methods in the Atmospheric Sciences*. Academic Press: London.

| | Correlation | | Parameter Stability | |
|---|---|---|---|---|
| Teleconnection | $r$ | $n$ | Chow Value | F-probability |
| $NINO3_{DJF}$-$CEP_{MAM}$ | +0.49 | 98 | 0.31 | 0.73 |
| $NINO3_{DJF}$-$NAP_{MAM}$ | -0.47 | 98 | 1.75 | 0.18 |
| $NINO3_{JJA}$-$NAP_{SON}$ | +0.24 | 98 | 0.78 | 0.46 |

Table 1: Probability values for correlation and temporal stability for lagged ENSO influences on European seasonal precipitation discussed herein. F-probabilities are computed by comparing regression parameters on two equal (1901-1949 and 1950-1998) subsets of the data.

| Parameter | Value | Standard Error | $p$-value |
|---|---|---|---|
| $a_0$ | 5440 | 1820 | 1% |
| $a_1$ | 10.4 | 2.0 | 0.1% |
| $a_2$ | -18.5 | 6.4 | 1% |

Table 2: Summary of parameter values from regression of $\text{NINO3}_{DJF}$ and $\text{LSST}_{DJF}$ onto $\text{CEP}_{MAM}$ using 1901-1998 data.

| | NINO3$_{DJF}$ and LSST$_{DJF}$ Model | | | NINO3$_{DJF}$ Model | | |
|---|---|---|---|---|---|---|
| Skill Measure for CEP$_{MAM}$ Precipitation | $n$ | Skill | 95% Confidence Interval | $n$ | Skill | 95% Confidence Interval |
| RMSE$_{cl}$ (%) | 30 | 18 | -3 to 34 | 30 | 16 | -4 to 32 |
| MAE$_{cl}$ (%) | 30 | 14 | -11 to 31 | 30 | 12 | -14 to 28 |
| PVE | 30 | 31 | 6 to 58 | 30 | 28 | 4 to 55 |

Table 3: Seasonal forecast skill for spring (MAM) precipitation over the central European area [45$^o$N to 55$^o$N, 35$^o$E to 5$^o$W] from winter (DJF) SSTs. Skill is assessed from true independent forecasts made over 30 years (1969-1998), and is shown for the three skill measures and the two forecast models discussed herein. The 95% confidence intervals are computed by bootstrapping 25,000 randomisations of the hindcast data.

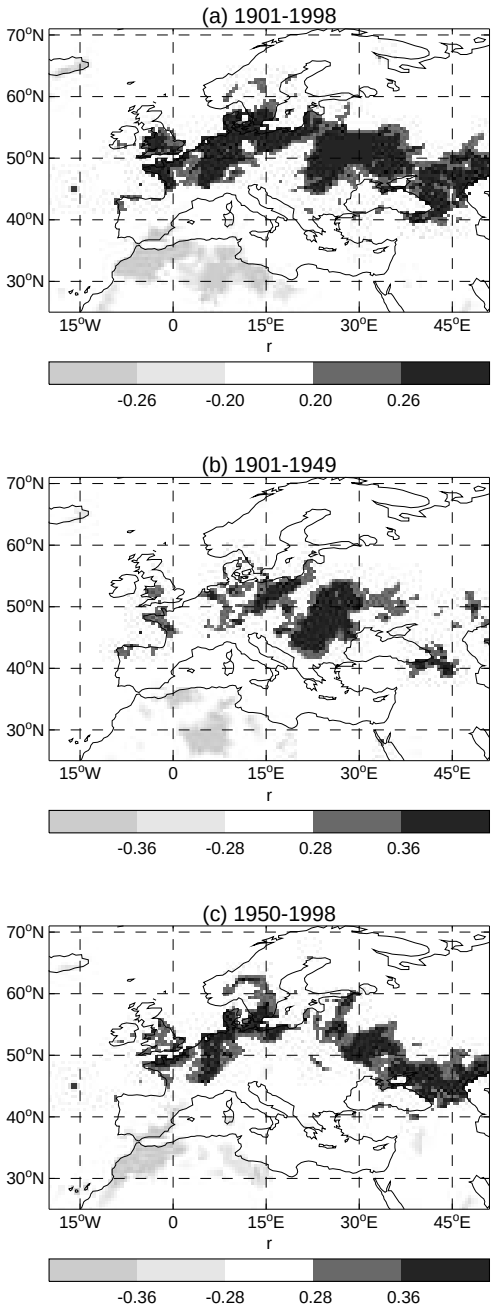


Figure 1: Maps of Pearson product moment correlation for NINO3$_{DJF}$ versus MAM precipitation (a) 1901-1998, (b) 1901-1949, and (c) 1950-1998. Shading shows the 5% and 1% significance levels.

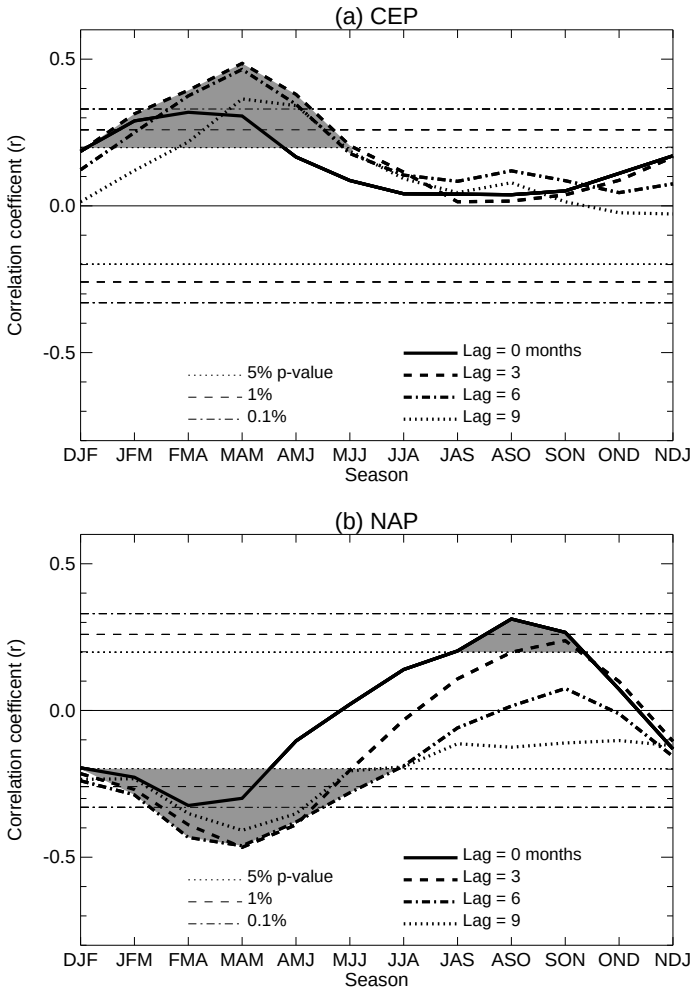


Figure 2: Correlation by season of (a) CEP, and (b) NAP versus NINO3$_{DJF}$ for lags of 0, 3, 6, and 9 months 1901-1998. Horizontal lines correspond to the 5%, 1%, and 0.1% p-values. Shading highlights the seasons where the lagged or contemporaneous ENSO influence on precipitation is significant at the 5% p-value or below.

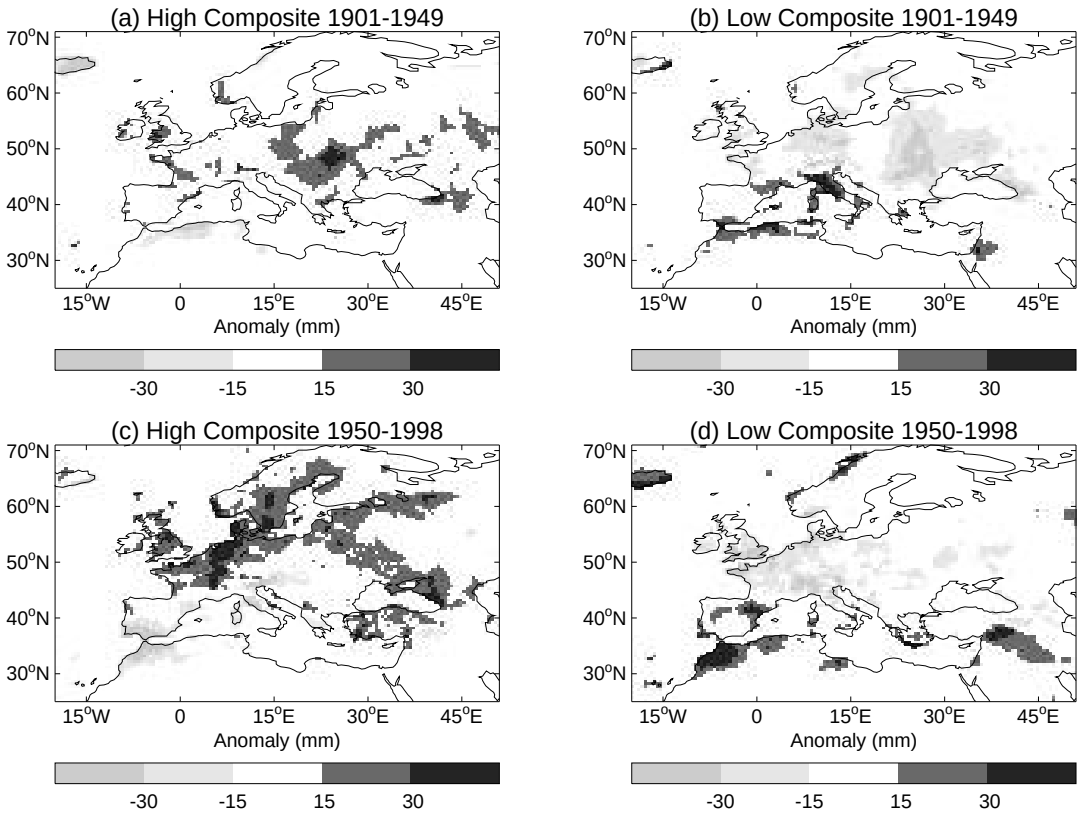


Figure 3: Spring precipitation anomalies corresponding to ENSO extremes. Each composite map displays the average MAM precipitation anomaly following the 10 most positive $\text{ENSO}_{DJF}$ winters (a) 1901-1949, (c) 1950-1998, and following the 10 most negative $\text{ENSO}_{DJF}$ winters (b) 1901-1949, (d) 1950-1998. Anomalies are calculated relative to the long term climatology (1901-1998).

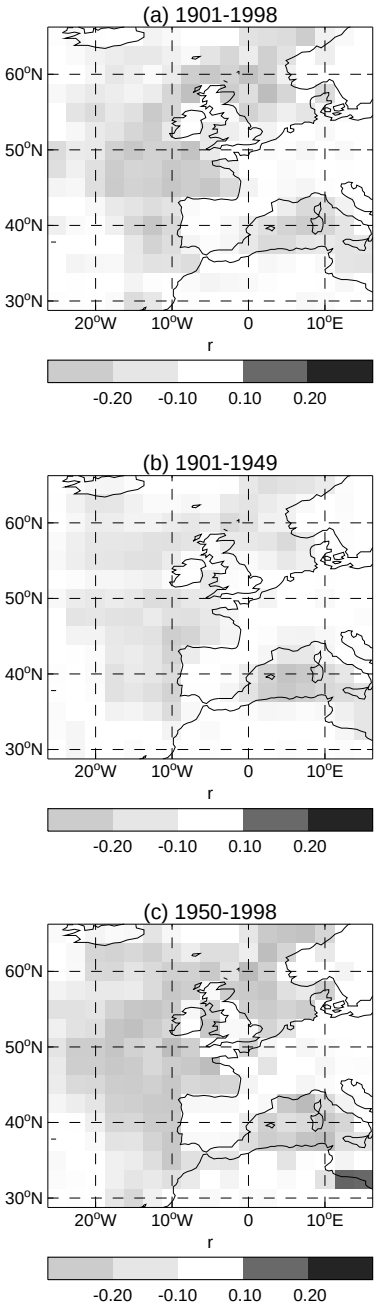


Figure 4: Maps of Pearson product moment correlation for $\mathrm{CEP}'_{MAM}$ versus local contemporaneous SST MAM (a) 1901-1998, (b) 1901-1949, and (c) 1950-1998.

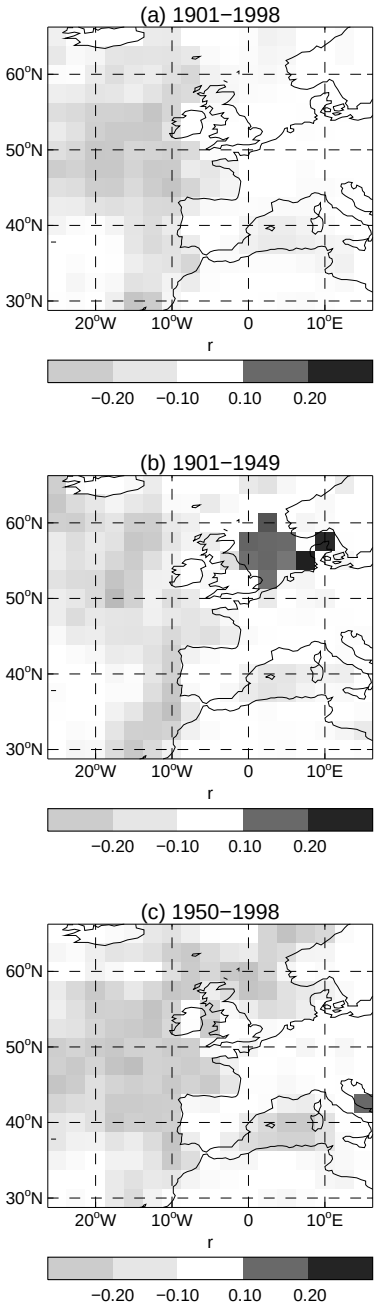


Figure 5: Maps of Pearson product moment correlation for $\mathrm{CEP}'_{MAM}$ versus local lagged SST DJF (a) 1901-1998, (b) 1901-1949, and (c) 1950-1998.

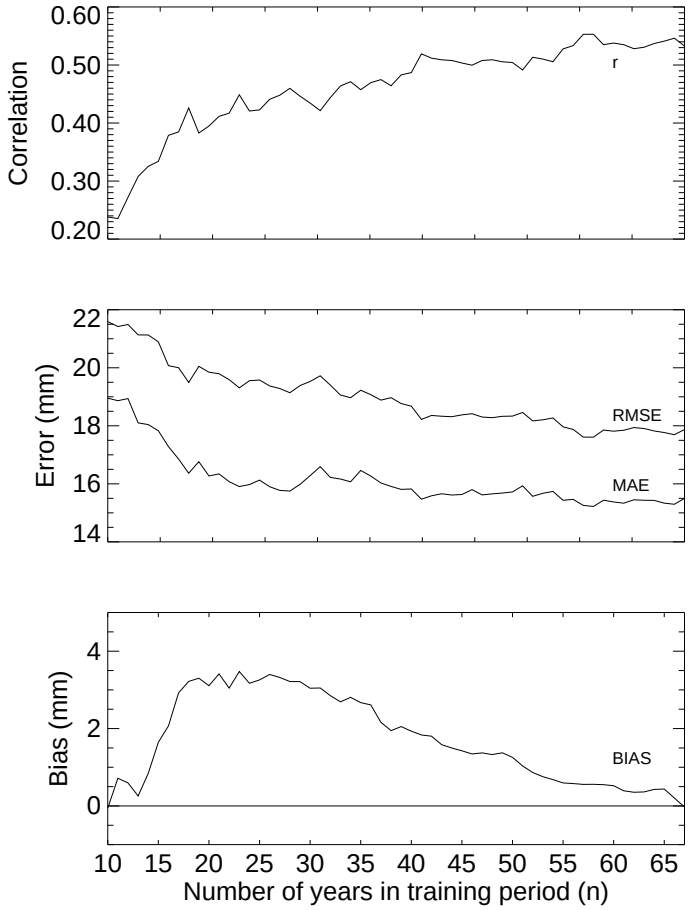


Figure 6: Hindcast performance for predicting $\text{CEP}_{MAM}$ from $\text{NINO3}_{DJF}$ and $\text{LSST}_{DJF}$ as a function of the number of years in the training period (n). All models are for the period 1969-1998 and only prior data are used in building the regressions. BIAS is bias, MAE is mean absolute error, RMSE is root mean square error, and $r$ is the correlation coefficient.

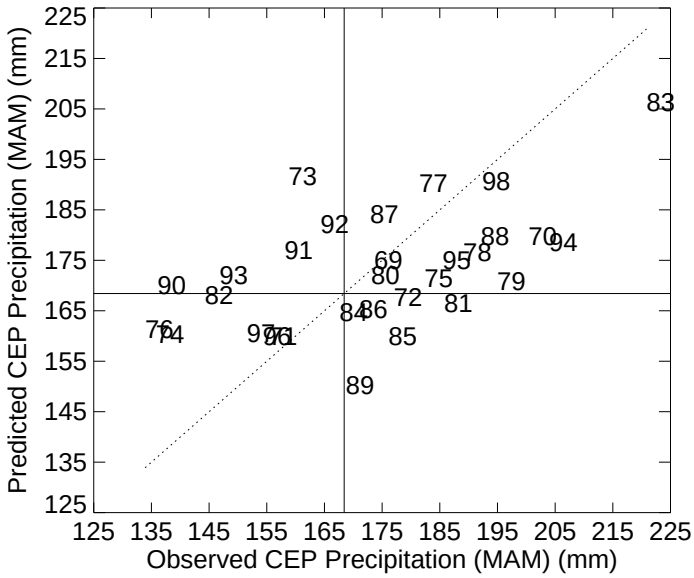


Figure 7: Scatter plot of hindcast results 1969-1998 for the prediction of $\text{CEP}_{MAM}$ from $\text{NINO3}_{DJF}$ and $\text{LSST}_{DJF}$ using data from 1901. Only data from years prior to the year being forecast are used in building the model. The horizontal and vertical lines represent the 1961-1990 climatology. The dotted line represents a perfect forecast.

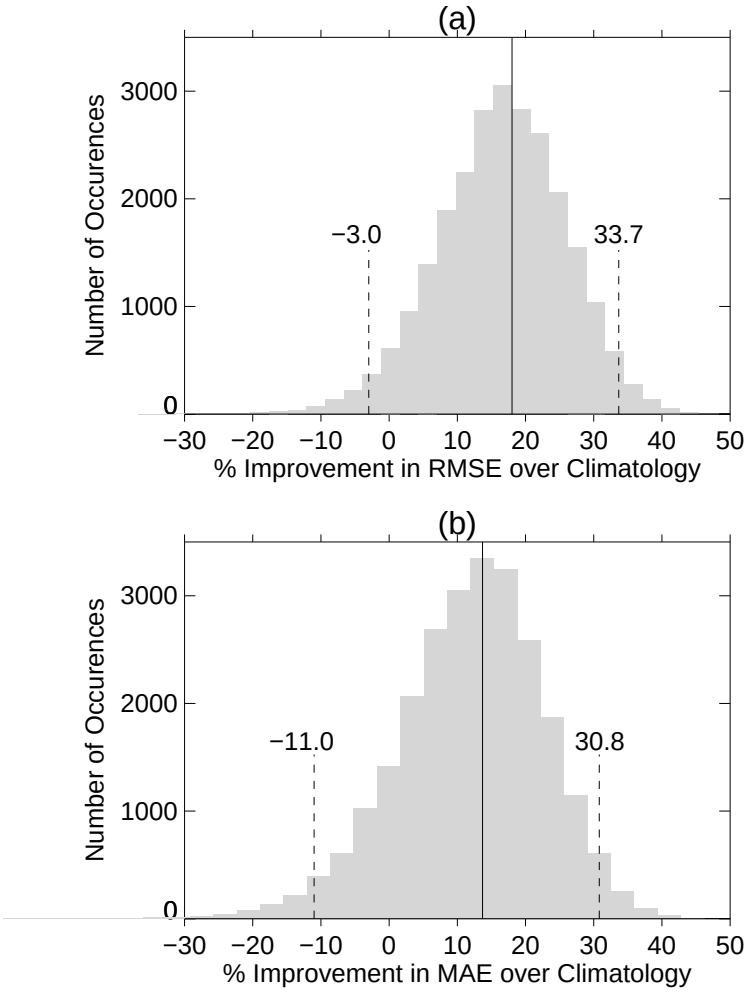


Figure 8: Bootstrapped skill score distributions for the hindcast period 1969-1998 based on (a) $\text{RMSE}_{cl}$, and (b) $\text{MAE}_{cl}$. The solid vertical line represents the point estimate of skill score, while the dashed lines mark the 95% two-tailed confidence interval.